Magneto-Raman Scattering of Graphene on Graphite: Electronic and Phonon Excitations

C. Faugeras,[1] M. Amado,[1,2] P. Kossacki,[1,3] M. Orlita,[1,4] M. Kühne,[1] A. A. L. Nicolet,[1] Yu. I. Latyshev,[5] and M. Potemski[1]

[1]*LNCMI, UPR 3228, CNRS-UJF-UPS-INSA, 38042 Grenoble, France*

[2]*QNS-GISC, Departamento de Física de Materiales, Universidad Complutense, E-28040 Madrid, Spain*

[3]*Institute of Experimental Physics, Faculty of Physics, University of Warsaw, Poland*

[4]*Institute of Physics, Faculty of Mathematics and Physics, Charles University, Ke Karlovu 5, 121 16 Praha 2, Czech Republic*

[5]*Kotelnikov Institute of Radio-Engineering and Electronics RAS, Mokhovaya 11-7, 125009 Moscow, Russia*

(Received 7 January 2011; published 14 July 2011)

Magneto-Raman-scattering experiments from the surface of graphite reveal novel features associated to purely electronic excitations which are observed in addition to phonon-mediated resonances. Graphene-like and graphite domains are identified through experiments with ~ 1 μm spatial resolution performed in magnetic fields up to 32 T. Polarization resolved measurements emphasize the characteristic selection rules for electronic transitions in graphene. Graphene on graphite displays the unexpected hybridization between optical phonon and symmetric across the Dirac point inter Landau level transitions. The results open new experimental possibilities—to use light scattering methods in studies of graphene under quantum Hall effect conditions.

DOI: 10.1103/PhysRevLett.107.036807 PACS numbers: 73.22.Lp, 63.20.kd, 78.30.Na, 78.67.−n

The effects of interactions, between electrons and/or electrons and phonons, turn out to be an emergent focus of the research on graphene [1]. These effects are particularly apparent when the magnetic field B is applied across the graphene plane and the continuous energy dispersion spectrum, $E = \pm v_F \mid \vec{p} \mid$, of this Dirac, two-dimensional system transforms into discrete Landau levels $L_{\pm n}$ with characteristic energies $E_{\pm n} = \pm v_F \sqrt{2e\hbar Bn}$ (where $\vec{p}$ is carrier momentum, $n = 0, 1, \ldots$, and v_F stands for the Fermi velocity). Magneto-Raman scattering is one possible spectroscopic tool to study the (selected) inter Landau level excitations, which is potentially sensitive to the effects of interactions [2,3].

So far, a search for the Raman scattering signal from (purely) electronic excitations between LLs of graphene systems [4–6] has been a veritable experimental challenge [7]. The dominant electronic resonances are predicted to be associated with the symmetric inter-LL transitions ($L_{-n} \rightarrow L_n$) across the 0th Landau level in the case of graphene [4,5] and of bilayer graphene [6]. Notably, however, the resonant hybridization of the E_{2g} optical phonon mode [8], with asymmetric $L_{-n,(-n-1)} \rightarrow L_{n+1,(n)}$ excitations [9], has been observed [10,11] and displayed a characteristic nature of electron-phonon interaction in graphene. If exfoliated graphene samples are often limited in quality or very fragile, the extremely pure graphene specimens which can be found on the surface of bulk graphite [12,13] might be more suitable for the refined spectroscopic studies [11] and investigations of both electronic and phonon-mediated response in magneto-Raman-scattering experiments.

In this Letter, we report on macro- and micro-magneto-Raman scattering experiments performed on natural graphite. Our results reveal a series of characteristic transitions which we assign as due to the electronic response and which are observed in addition to previously studied, phonon-mediated excitations. A mixture of graphene and graphite response is seen in macro experiments. By scanning the sample surface with micro-Raman scattering at high fields, we localize the graphene flakes on graphite substrate [11] via mapping the E_{2g} magneto-phonon resonance. Focusing on such a location we experimentally identify the dominant features in the electronic Raman scattering response of graphene, which, in agreement with theoretical predictions, arise from symmetric, across the Dirac point, inter Landau level excitations. Strikingly, and beyond the existing theoretical models, these symmetric excitations also couple to the optical phonon E_{2g} mode. Electron-electron interactions and/or symmetry breaking effects due to interaction with the substrate are speculated to be among the possible causes of this effect.

Raman-scattering spectra were measured using the Ti:sapphire laser setup, tuned at accurately controlled wavelength in the range $\sim\lambda = 720$ nm, in order to minimize the superfluous Raman signal of optical fibers. The sample was immersed in a helium gas kept at $T = 4.2$ K and placed in a resistive magnet delivering fields up to 32 T. The nonpolarized Raman scattering spectra were measured in nearly backscattering Faraday geometry. The collected light was dispersed with a single grating spectrometer (spectral resolution $\Delta\lambda = 0.3$ nm) equipped with nitrogen cooled CCD detector and band pass filters were used to reject the stray light. For macro-Raman-scattering experiments, an experimental setup similar to the one described in Ref. [10] was used with a laser spot of 600 μm-diameter and an optical power $\sim$100 mW. For micro-Raman measurements, a monomode fiber with a core of 5 μm diameter was used for optical excitation and a 200 μm core

optical fiber was used for collection. Aspherical lenses were used for excitation and collection. The laser spot on the sample was ~ 1 μm and an optical power of 5 mW was used for excitation. The sample has been mounted on a X-Y-Z piezzo stage allowing us to move the sample with respect to the laser spot with a spatial resolution better than 1 μm.

The results of our macro-Raman-scattering measurements are summarized in Fig. 1 which shows a false-color plot of spectra with subtracted $B = 0$ response, measured in the spectral range of the vicinity of the E_{2g} optical phonon energy, as a function of the magnetic field. Different series of magnetic field dependent features can be distinguished, with different intensities and different behaviors when tuned in resonance with the E_{2g} optical phonon energy.

Two $L_{-n,n}$ and $L^{-n-1,n}_{-n,n+1}$ series of features scale with $\sqrt{B}$ and can be associated with transitions which involve Landau levels L_n of massless Dirac fermions with Fermi velocity $v_F = 1.02 \times 10^6$ m s^{-1}. The better pronounced $L_{-n,n}$ series is due to symmetric, $L_{-n} \rightarrow L_n$ transitions whose energies are reproduced with the calculated solid lines in Fig. 1. These transitions are expected to dominate the electronic magneto-Raman scattering response of graphene [4]. The overall weaker $L^{-n-1,n}_{-n,n+1}$ series is due to asymmetric $L_{n,(-n-1)} \rightarrow L_{n+1,(n)}$ LL transitions (optical-like excitations) which, on the other hand, give rise to the pronounced magnetophonon resonance. Dotted lines in Fig. 1 represent the coupled, optical phonon-electronic excitations as defined in Ref. [9] for neutral graphene and calculated with an electron-phonon coupling constant of 3000 ± 50 cm^{-1} [10,14].

The third $L^b_{-n,n}$ series of features which scale more linearly with the magnetic field is here attributed to the Raman scattering response arising from massive electrons at the K point of graphite [15,16]. The in plane dispersion of these electronic states can be well approximated by the one of the effective bilayer graphene with the interlayer coupling γ_1 enhanced by a factor of 2 with respect to a true bilayer graphene [17–20]. The $L^b_{-n,n}$ features can be therefore identified with the symmetric $L^b_{-n} \rightarrow L^b_n$ transitions between LL levels of such an effective bilayer graphene. Energies, E^b_n, of these levels are given by

$$E^b_n = \mathrm{sgn}(n)\frac{1}{\sqrt{2}}[(2\gamma_1)^2 + (2n+1)E_1^2 - \sqrt{(2\gamma_1)^2 + 2(2n+1)E_1^2(2\gamma_1)^2 + E_1^4}]^{1/2},$$

where $E_1 = v_F\sqrt{2e\hbar B}$ and energies of $L^b_{-n} \rightarrow L^b_n$ transitions are $2E^b_n$. Those latter values have been calculated assuming that $\gamma_1 = 375$ meV (and $v_F = 1.02 \times 10^6$ m s^{-1}) and are plotted in Fig. 1 with dashed lines which coincide well with the measured $L^b_{-n,n}$ transitions. Although we are not aware of any theoretical works on magneto-Raman scattering response of bulk graphite, the predictions regarding the bilayer graphene are in line of our identification of the $L^b_{-n} \rightarrow L^b_n$ excitations. Notably those transitions are very likely the same as previously reported [7] but interpreted differently.

More striking is our observation of the series of the L-type, graphenelike transitions. One could speculate that these transitions arise due to electronic states at the H point of graphite, which to some extent also reflect the behavior of massless Dirac fermions [19]. The origin of these transitions is however different as we elucidate this with micro-magneto-Raman-scattering experiments. In Fig. 2(a) we present two micro-Raman-scattering spectra, both measured at $B = 20$ T but at two different locations on the surface of natural graphite. When the laser spot is at location B, the E_{2g} optical phonon appears clearly as a two-components feature indicating an efficient electron-phonon coupling, similar to the one discussed in Ref. [10]. In contrast, at the location A, the E_{2g} optical phonon appears

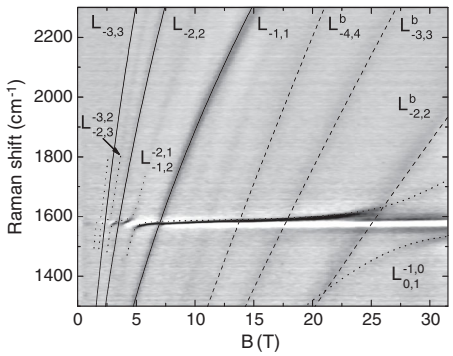

FIG. 1. False-color map of the $B = 0$ T spectrum subtracted macro-Raman spectra of natural graphite as a function of the magnetic field. Dotted lines are the graphene-optical phonon coupled modes discussed in Ref. [9], solid lines are the calculated symmetric inter Landau level transitions $L_{-n,n}$ in graphene, dashed lines are the symmetric transitions $L^b_{-n,n}$ in the effective bilayer. All these lines are calculated with a Fermi velocity $v_F = 1.02 \times 10^6$ m s^{-1} and $2\gamma_1 = 750$ meV.

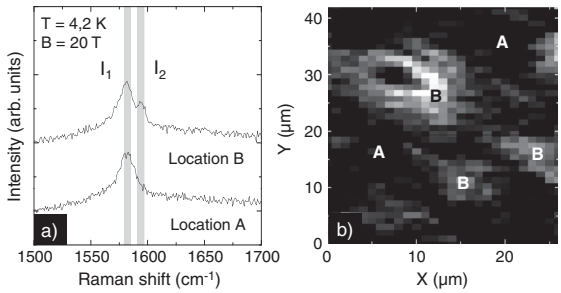

FIG. 2. (a) Unpolarized micro-Raman scattering spectra at $B = 20$ T for two different representative locations on the surface of natural graphite. The shaded area represent the energy interval from which the average amplitude I_1 and I_2 are extracted. (b) False-color map of the intensity ratio I_1/I_2 showing different regions on the surface of natural graphite. At $B = 20$ T, the E_{2g} phonon appears as a single component feature in locations A, as a two-components feature in locations B.

as a single component feature pointing towards a much weaker effect of electron-phonon coupling. Let us define I_1 as the amplitude of the scattered light at the E_{2g} optical phonon energy and I_2 as the amplitude of the scattered light at the energy where the second component appears [see Fig. 2(a)]. In Fig. 2(b) we present a false-color map of the ratio $R = I_1/I_2$ as a function of the position of the excitation spot on the surface of the sample. In regions of high R (dark regions in Fig. 2(b)], the E_{2g} optical phonon appears as a single component feature [A spectrum in Fig. 2(a)] while low R indicates regions where the E_{2g} optical phonon appears as a double component feature [light gray regions labeled B in Fig. 2(b)]. The surface of natural graphite is therefore not homogeneous. A regions display predominantly the excitations characteristic of massive carriers at the K point of the band structure of bulk graphite. The magneto-Raman spectra from such locations will be discussed in more details elsewhere.

Here we focus on B locations, of few square micrometers, which we identify as graphene inclusions (decoupled graphene flakes) on the surface of the bulk graphite [12,13]. Indeed, as shown in Fig. 3, the Raman scattering response measured with micron resolution from the B location is practically free of L^b graphite features. The remaining L-type transitions are characteristic of graphene and are not observed when placing the laser spot on A locations. Solid and dotted lines in Fig. 3 are the corresponding traces redrawn from Fig. 1 and they reflect well the overall behavior of the observed transitions, which can be now analyzed in more details.

To further elucidate the nature of the electronic $L_{-n,n}$ transitions, we have performed polarization resolved experiments at low magnetic fields. As shown in Fig. 4, they can be observed far away from the E_{2g} phonon resonance. Moreover, the $L_{-n,n}$ symmetric transitions imply no change of angular momentum and, in accordance to theoretical predictions [4], are seen when the helicity of the circularly polarized incoming light and of the outgoing scattered signal are the same. In contrast, the optical phonon with the E_{2g} symmetry [4,9] dominates the spectra in crossed polarization configuration. The relative intensity of these electronic features with respect to the one of the phonon feature strongly depends on the location on the sample.

Finally, let us turn our attention on the close vicinity of the E_{2g} phonon signal and focus carefully on its behavior at low magnetic fields, below 8 T. Figure 5(a) shows a false-color map of the unpolarized Raman spectra with subtracted $B = 0$ spectrum and Fig. 5(b) illustrates the field dependence of $\rho(B)$, the amplitude of the Raman scattering signal at the energy which corresponds to the center of the E_{2g} peak measured at zero magnetic field (1582.2 cm^{-1}) and scaled with respect to its zero field value. As expected, this trace shows minima, marked by solid lines in Fig. 5(a), which appear at magnetic fields at which the energies of $L_{-n-1,(-n)} \rightarrow L_{n,(n+1)}$ transitions coincide with the E_{2g}-phonon energy. These minima are the result of regular magneto-phonon effect [8–11] which de facto implies an avoided crossing between those asymmetric LL transitions and the optical phonon mode. Surprisingly, the $\rho(B)$ dependence shows another set of well pronounced minima, marked by dashed lines in Fig. 5(b) (The behavior of $\rho(B)$ above 8 T is reflecting the shift of the phonon line towards higher energies). They clearly appear when the symmetric $L_{-n} \rightarrow L_n$ transitions are tuned in resonance with the E_{2g}-phonon. We therefore deduce and illustrate it more clearly in Fig. 5(b) that both asymmetric and symmetric inter Landau level transitions show the effect of avoided crossing with the E_{2g} phonon mode. To be more quantitative, we have simulated the coupling of both asymmetric and symmetric LL transitions to the phonon mode [see Fig. 5(a)]. In case of asymmetric transitions, we have repeated the calculations according to the prescription of Ref. [9], in which the coupling parameters for each resonance grow with magnetic field and are determined by the strength (3000 ± 50 cm^{-1}) of electron-phonon interaction. In case of symmetric transitions we have

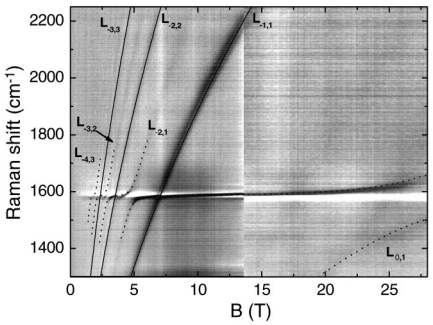

FIG. 3. False-color map of the $B = 0$ T spectrum subtracted micro-Raman spectra measured with the laser spot on location B as a function of the magnetic field. Solid lines correspond to symmetric transitions $L_{-n,n}$ in graphene while dotted lines correspond to the hybrid modes involving E_{2g} phonons and optical-like transitions in graphene.

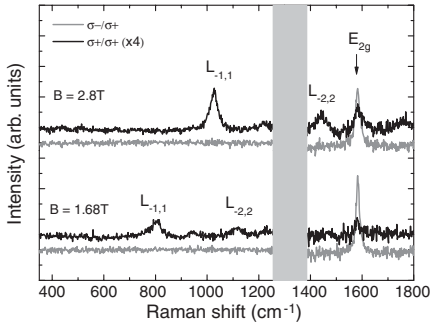

FIG. 4. Micro-Raman-scattering spectra measured at a B-location at $B = 1.68$ T and 2.8 T at $T = 4.2$ K in the $\sigma+/\sigma-$ (gray curves) and in the $\sigma+/\sigma+$ (black curves x4) polarization configurations (excitation or detection) showing two purely electronic Raman scattering features $L_{-1,1}$ and $L_{-2,2}$. The shaded region is due to a magnetic field dependent background feature affecting the spectra.

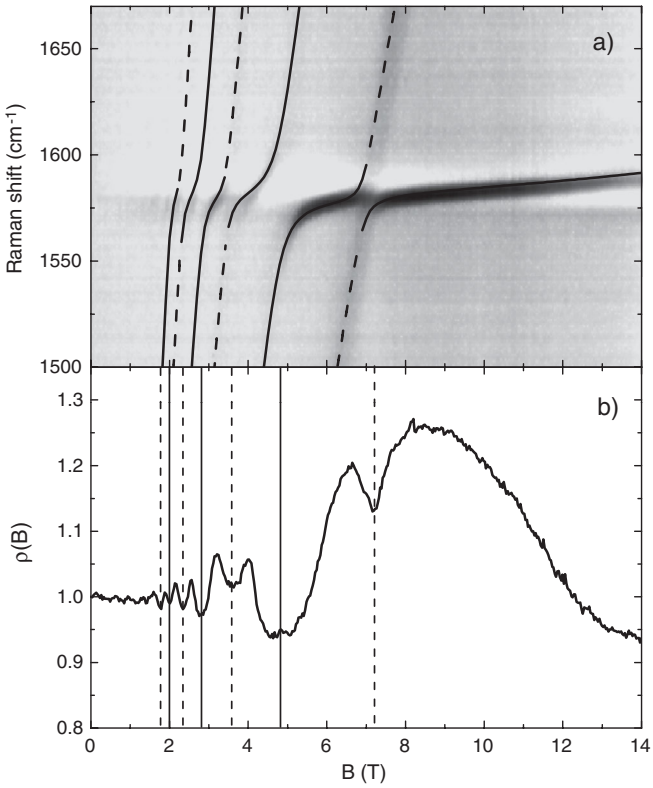

FIG. 5. (a) False-color map of the $B = 0$ T spectrum subtracted Raman scattering spectra in the E_{2g} phonon range of energy. The solid and dashed lines represent optical and symmetric electronic excitations coupled to optical phonons. (b) $\rho(B)$, amplitude of the Raman scattering response at the E_{2g} phonon energy (1582.2 cm^{-1}) normalized to the zero field amplitude, as a function of magnetic field. Solid lines represent the resonant fields of optical-like transitions with the E_{2g} phonon while dotted lines are the resonant fields of symmetric transitions with the E_{2g} phonon.

phenomenologically introduced the coupling parameters, separately for each resonance, and found $\delta = 4.7$, 11.1, and 15.7 cm^{-1} for the resonances of the E_{2g}-phonon with correspondingly $L_{-1,1}$, $L_{-2,2}$, and $L_{-3,3}$ transitions which appear at $B = 7.19$, 3.61, and 2.31 T, respectively. The decreasing with magnetic field strength makes us speculate that it originates from the mixing of wave functions of neighboring Landau levels. Such mixing may result from Coulomb, electron-electron interactions [21]. It is however surprising that the couplings involving symmetric lines observed at low magnetic fields, are as strong as the standard magneto-phonon effect. Notably, graphene on graphite may consist of rotationally twisted sheet with respect to Bernal-stacked underneath layers. The role of substrate, and possible other symmetry breaking effects cannot be *a priori* excluded. We believe our observation will trigger pertinent theoretical studies which are beyond the scope of our experimental paper.

Concluding, we have presented low temperature macro and micro-Raman scattering experiments in magnetic fields performed on natural graphite, which show the existence of graphene flakes decoupled from bulk graphite and which reveal the rich electronic excitation spectrum of graphene. We have determined the different polarization selection rules for these excitations. The magneto-phonon effect of undoped graphene is revealed as well as a coupling of electronic transitions symmetric across the Dirac point and the optical phonon. This coupling is observed because of the mixing of Landau levels wave functions. The origin of this mixing remains unknown what calls further theoretical works on electron-phonon coupling in graphene. Our observation of electronic response in magneto-Raman scattering from graphene opens new possibilities to studying the properties of this new quantum Hall effect system.

We would like to acknowledge fruitful discussions with D. M. Basko and V. I. Falko. Part of this work has been supported by ANR-08-JCJC-0034-01, GACR P204/10/1020, GRA/10/E006 (EPIGRAT), RTRA "DISPOGRAPH" projects and by EuroMagNET II under the EU Contract No. 228043. P. K. is financially supported by the EU under FP7, Contract No. 221515 ''MOCNA''. Yu. L. is supported by the Russian state Contract No. 16.740.11.0146.

[1] A. K. Geim, Science **324**, 1530 (2009).
[2] A. Pinczuk *et al.*, Phys. Rev. Lett. **68**, 3623 (1992).
[3] A. B. Van'kov *et al.*, arXiv:1011.2022.
[4] O. Kashuba and V. I. Fal'ko, Phys. Rev. B **80**, 241404(R) (2009).
[5] R. Roldan *et al.*, Semicond. Sci. Technol. **25**, 034005 (2010).
[6] M. Mucha-Kruczynski, O. Kashuba, and V. I. Falko, Phys. Rev. B **82**, 045405 (2010).
[7] A. F. Garcia-Flores *et al.*, Phys. Rev. B **79**, 113105 (2009).
[8] T. Ando, J. Phys. Soc. Jpn. **76**, 024712 (2007).
[9] M. O. Goerbig *et al.*, Phys. Rev. Lett. **99**, 087402 (2007).
[10] C. Faugeras *et al.*, Phys. Rev. Lett. **103**, 186803 (2009).
[11] J. Yan *et al.*, Phys. Rev. Lett. **105**, 227401 (2010).
[12] G. Li, A. Luican, and E. Y. Andrei, Phys. Rev. Lett. **102**, 176804 (2009).
[13] P. Neugebauer *et al.*, Phys. Rev. Lett. **103**, 136403 (2009).
[14] J. Yan *et al.*, Phys. Rev. Lett. **98**, 166802 (2007).
[15] J. C. Slonczewski and P. R. Weiss, Phys. Rev. **109**, 272 (1958).
[16] J. W. McClure, Phys. Rev. **104**, 666 (1956).
[17] M. Koshino and T. Ando, Phys. Rev. B **77**, 115313 (2008).
[18] M. Orlita *et al.*, Phys. Rev. Lett. **100**, 136403 (2008).
[19] M. Orlita *et al.*, Phys. Rev. Lett. **102**, 166401 (2009).
[20] K. -C. Chuang, A. M. R. Baker, and R. J. Nicholas, Phys. Rev. B **80**, 161410(R) (2009).
[21] R. Roldan, J. N. Fuchs, and M. O. Goerbig, Phys. Rev. B **82**, 205418 (2010).